



A Novel Skeleton Extraction Algorithm for 3d Wireless Sensor Networks

By S. K. Pushpa, S. Ramachandran & K. R. Kashwan

Vinayaka Missions University, India

Abstract - Wireless sensor network design is critical and resource allocation is a major problem which remains to be solved satisfactorily. The discrete nature of sensor networks renders the existing skeleton extraction algorithms inapplicable. 3D topologies of sensor networks for practical scenarios are considered in this paper and the research carried out in the field of skeleton extraction for three dimensional wireless sensor networks. A skeleton extraction algorithm applicable to complex 3D spaces of sensor networks is introduced in this paper and is represented in the form of a graph. The skeletal links are identified on the basis of a novel energy utilization function computed for the transmissions carried out through the network. The frequency based weight assignment function is introduced to identify the root node of the skeleton graph. Topological clustering is used to construct the layered topological sets to preserve the nature of the topology in the skeleton graph.

Keywords : 3d, algorithm, protocol, wireless sensor networks, skeleton extraction, skeleton node.

GJCST-E Classification : C.2.1



Strictly as per the compliance and regulations of:



A Novel Skeleton Extraction Algorithm for 3d Wireless Sensor Networks

S. K. Pushpa ^α, S. Ramachandran ^σ & K. R. Kashwan ^ρ

Abstract- Wireless sensor network design is critical and resource allocation is a major problem which remains to be solved satisfactorily. The discrete nature of sensor networks renders the existing skeleton extraction algorithms inapplicable. 3D topologies of sensor networks for practical scenarios are considered in this paper and the research carried out in the field of skeleton extraction for three dimensional wireless sensor networks. A skeleton extraction algorithm applicable to complex 3D spaces of sensor networks is introduced in this paper and is represented in the form of a graph. The skeletal links are identified on the basis of a novel energy utilization function computed for the transmissions carried out through the network. The frequency based weight assignment function is introduced to identify the root node of the skeleton graph. Topological clustering is used to construct the layered topological sets to preserve the nature of the topology in the skeleton graph. The skeleton graph is constructed with the help of the layered topological sets and the experimental results prove the robustness of the skeleton extraction algorithm introduced. Provisioning of additional resources to skeletal nodes enhances the sensor network performance by 20% as proved by the results presented in this paper.

Keywords: 3d, algorithm, protocol, wireless sensor networks, skeleton extraction, skeleton node.

I. INTRODUCTION

Wireless sensor networks constitute sensor nodes that are deployed over a topological area. Sensor nodes are independent, low resource devices possessing processing units, sensing devices, communication bandwidth, power resources and radio trans-receiver systems. Network life time, accurate data aggregation, and overhead reduction are desired characteristics of sensor network deployments. Network design is critical to construct efficient wireless sensor networks. Sensor networks are used for varied applications like unforeseen disaster relief [1] and [2], underwater sensor networks [3], monitoring activities [4], surveillance in military applications [5], medical monitoring systems [6] and many more. Network design is critical in sensor network deployments to achieve the desired goals [7]. Considering the varied application domain of sensor networks, it can be stated that the

deployment methodology and the geographic deployment environments greatly vary. Wireless sensor network design, deployments of sensor nodes and analyzing the resources to be allocated to the sensor nodes is a major problem that exists. The shape of wireless sensor network deployments generally considered are usually in the shapes of a square or oval which is not the case in actual deployments [8].

Moreover researchers generally consider 2D topologies or 3D projections schemes to model the surface coverage which lead to inaccuracies and deviations from realistic environments [9]. In real word applications, sensor network deployments are complex 3D spaces. Generally researchers use a simple 2D ideal plane [10, 11] or a 3D full space models [12, 13] for the environment which are inadequate to achieve realistic results. A recent study conducted by Linghe Kong et al. [9] highlights the surface coverage problems for deployments of sensor networks in the idealistic world. In Ref. [9], the authors ascertain that the field of interest is neither 2D nor 3D but consists of complex surfaces, with the help of the Tungurahua volcano monitoring project [14] shown in Fig. 1. Furthermore, the authors in Ref. [9] define a coverage dead zone that exists in adopting a 2D surface coverage model described in Fig. 2 of this paper. Let us consider a set of seven sensor nodes termed Node A – Node G as shown in Fig. 3. The sensor nodes appear to be deployed in an elevated 3D terrain or a hill sort of a terrain. The 2D representation of the similar topology is presented in Fig. 4. While considering 2D topologies, nonexistent or impractical links are established as shown by a thick grey line in the figure. This error generally occurs in the network and the physical layer modeling.

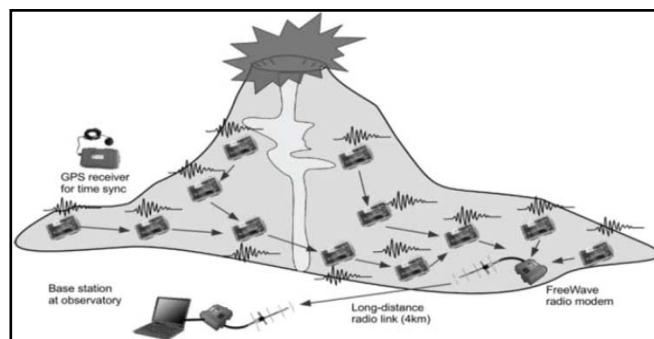


Figure 1 : Volcano monitoring Project from Harvard Sensor Networks Lab [14]

Author ^α: Vinayaka Missions University, Salem, India.

e-mail: skpushpamurtheppa@yahoo.com

Author ^σ: S J B Institute of Technology, Bangalore, India.

e-mail: ramachandr@gmail.com

Author ^ρ: Sona College of Technology, Salem, India.

e-mail: drkrkashwan@gmail.com

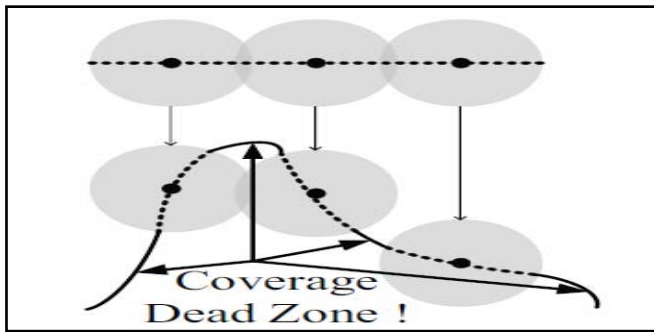


Figure 2: Coverage Problem Dead Zone that occurs when 2D Plane Solutions are adopted to 3D surfaces [9]

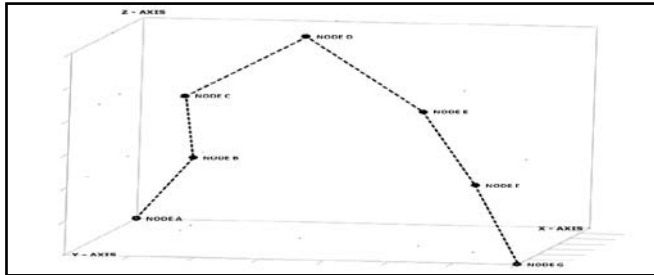


Figure 3: A seven sensor node topology in 3D surface

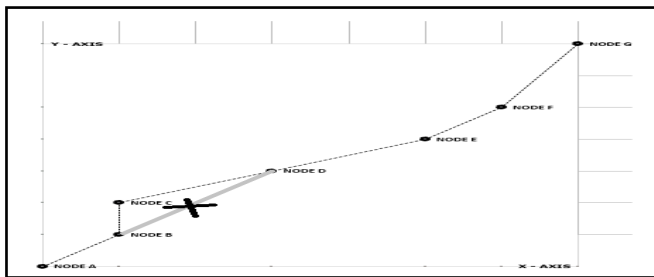


Figure 4: Network Layer/Radio Layer Error while applying 2D models to 3D topologies of Sensor Networks

From the above mentioned examples, it is evident that the 2D models that currently exist may not be applicable to real world scenarios. In the research work presented, the authors propose to consider 3D complex surface models for modeling sensor network deployments.

Skeleton extraction techniques have been extensively studied in the areas of image processing [15], medical image processing [16], computer graphics [17] and computer vision [18] and [19]. The use of skeleton extraction to represent the shape properties is well established. The skeleton extraction algorithms discussed above cannot be directly applied to wireless sensor network topologies as wireless sensor network topologies are discrete in nature and not continuous. Also the skeleton of wireless sensor networks depends on the network connectivity of the sensor nodes and not on the topological position alone. Wireless sensor networks are noisy by nature owing to the fact that the hop based approach is used to compute distances and not the Euclidean distance. The effect of noise tends to

inaccurate skeleton extraction proved in Ref. [21]. In post skeleton node identification, the skeleton node connectivity also poses another challenge as the skeleton connectivity is physical layer based and not discrete. The use of skeleton extraction techniques to represent wireless sensor network topologies and thus enhance the performance is proposed by researchers in Ref. [20-22]. However, the application to the 3D topologies is still limited. The research work presented here considers sensor network deployments in 3D complex spaces.

This paper introduces a skeleton extraction algorithm applicable to 3D wireless sensor network topologies where the coverage of the network is considered as a complex 3D function. In order to extract the skeleton, transmissions are initiated from each sensor node to all the other sensor nodes recursively and are modeled as transmission vectors. An energy utilization function is defined to identify the skeletal links. The skeleton is represented as a graph and the root node is computed using the frequency based weight assignment function. The skeleton nodes are extracted from the skeletal links. The skeleton graph construction is achieved by layered topological sets that represent decomposed clusters of the topology. The distance function is defined to organize the position of the skeleton nodes in the skeleton graph.

The remaining manuscript is organized as follows. The literature is reviewed in section two of this paper. The proposed skeleton extraction algorithm is presented in the third section. The experimental study is described in the subsequent section. The conclusions of the research work are drawn in the last section of this paper.

II. LITERATURE REVIEW

The skeleton extraction algorithms proposed by researchers can be broadly classified into four categories namely thinning and boundary propagation, distance field-based, geometric based, and general-field function based methods [18]. In the thinning and boundary based methods, the skeleton is represented as a thin line describing the topology. It is usually achieved by recursively shrinking of objects to a core thin line representing the topology [23]. To reduce the processing time which is a major drawback of the thinning and boundary based methods, researchers have also proposed parallel implementations of the thinning algorithms in 3D objects [24]. Most of the distance field based algorithms adopt a three step approach to extract the skeleton. The primary step constitutes in obtaining the ridge points of the object. Then a pruning methodology is applied followed by the connectivity phase to construct the skeleton. For connectivity, many algorithms like the shortest path technique [25, 26], minimum spanning tree [27, 28], LM path technique [29] or other geometric techniques are

utilized. The advantage of distance field methods is that they are computationally lighter when compared to the other methods and is very effective in the case of tubular objects. The major drawback of the distance field algorithms is that on application to arbitrary objects, the skeleton extraction is not accurate. In the geometric based methods of skeleton extraction the objects are represented as sets of scatter points or structures of polygonal meshes. Voronoi diagram representations [30-32] is a popular example for geometric based methods for skeleton extraction. The polyhedral geometric method to represent 3D structures is discussed in Ref. [33, 34]. The drawbacks of the geometric methods are that they are computationally more expensive when compared to the thinning and boundary based methods and they produce medial surfaces rather than the skeleton curve. In the general field generation based methods, varied functions are utilized to represent fields and these functions are utilized to generate skeleton curves. Potential field functions [35, 36], visible repulsive force functions [37], electrostatic field functions [38], radial basis functions [39] are a few considered by researchers. The field generation algorithms are less sensitive to noise and produce better results when compared to the geometric methods. As the field generation functions are first or second order functions, they are computationally heavy to solve and are considered unstable. The skeleton extraction methodologies may not be applicable to wireless sensor network topologies directly, which is the purpose of the research work proposed here.

Skeleton extraction in wireless sensor networks pose many challenges as discussed in the previous section of the paper. The migration of topology shapes to geometrical ones and the use of a dynamic medial axis model to present these geometric shapes are used for skeleton extraction in Ref. [40]. A medial axis based naming and routing protocol for wireless sensor networks is proposed in Ref. [21]. The methodology proposed in Ref. [21] consists of two protocols, namely, the medial axis construction protocol and the medial axis based routing protocol. In the medial axis construction protocol, the skeleton nodes are identified and the skeleton of the wireless sensor network topology is constructed. The medial axis based routing protocol achieves efficient load distribution during routing through the sensor networks due to the local decision capacities while routing. In Ref. [8], a connectivity based skeleton extraction algorithm applicable to wireless sensor network topologies is proposed. The coarse skeleton graph is extracted by boundary partitioning to identify the skeletal sensor nodes, generating the skeletal arcs, extending connectivity amongst the skeletal arcs. This coarse skeleton is finally refined to give the skeleton graph. The algorithm proposed in Ref. [8] accurately preserves the network topology and is robust to the noisy sensor

network topology. A distance transform based skeleton extraction algorithm for large scale wireless sensor networks is proposed in Ref. [22]. The algorithm proposed by Wenping Liu et al. [22] is more applicable to the practical applications as it does not require accurate or complete boundaries of sensor network topologies, exhibits lower communication overheads and is robust to noise. In Ref. [22], the coarse skeleton is generated by constructing the node map based distance transform of the sensor network; using the distance map the skeleton nodes are identified and the arcs are connected using a controlled folding scheme. The coarse skeleton is refined using the shortest path trees to construct the skeleton graph. The drawbacks of the skeleton extraction algorithms for wireless sensor networks discussed here is that the authors have considered the surface coverage in only 2D topologies and not the complex 3D topologies of wireless sensor networks that practically exist and proved in Ref. [9].

III. PROPOSED SYSTEM - SKELETON EXTRACTION ALGORITHM FOR 3D WIRELESS SENSOR NETWORKS

a) Preliminary Notations

Let us consider a 3D wireless sensor topology \mathcal{T} be represented as a graph $\mathbb{G}(N, L)$, where N represents the sensor node set and L is the wireless link set. The location wireless sensor node $n_a \in N$ described by Cartesian coordinates is represented by

$$p_{n_a} = (x_{n_a}, y_{n_a}, z_{n_a}) \quad (1)$$

The skeleton or critical nodes to be identified in the sensor network topology \mathbb{G} is defined by a set S and the remaining nodes are defined by the set R .

$$N = S \cup R \quad (2)$$

Let the transmission radius of the sensor node be represented as r_t and the sensing radius be represented as r_s . As 3D topologies in complex spaces are considered, the coverage of the N sensor nodes [9] can be defined as

$$1 - \left(1 - \sum_i ((\mathcal{A}_i/\mathcal{A}_{\mathcal{T}})(2\pi^2 r^2/2\pi(\pi r^2 + \mathcal{A}_i) + 2\pi r \mathcal{A}_i)((\mathcal{A}_i + \mathcal{P}_i r + \pi r^2) \cos \theta_i / (\mathcal{A}'_{\mathcal{T}} + \mathcal{P}_{\mathcal{T}} r + \pi r^2))) \right)^{\lambda(\mathcal{A}'_{\mathcal{T}} + \mathcal{P}_{\mathcal{T}} r + \pi r^2)} \quad (3)$$

Where $\mathcal{A}_{\mathcal{T}}$ represents the area
 $\mathcal{P}_{\mathcal{T}}$ is the perimeter
 λ is the sensor deployment intensity
 θ_i is the angle between \mathcal{A}_i and $x y$ plane and
 $\mathcal{A}'_{\mathcal{T}}$ is the area of the z plane projection of \mathcal{A}_i .

The skeleton of the 3D wireless topology \mathcal{T} can be considered to represent a graph $\mathbb{G}_S(S, L_S)$, where $\mathbb{G}_S \subset \mathbb{G}$ and L_S is a set of skeleton links amongst S_E and S_C . S_E represents the set of the extreme sensor nodes in the topology \mathcal{T} and S_C represents the sensor node which is common to all the skeleton links L_S . In order to extract the skeleton of sensor networks generally a transmission based scheme is adopted [41] [42], in which each sensor node initiates a transmission to the other nodes and then the response messages or the route reply messages are used to derive \mathbb{G}_S and hence the authors of this paper adopt a similar mechanism. The major drawback of such mechanisms already adopted is that the network energy utilized associated with the transactions is established heuristically and are not applicable to 3D sensor

networks. In order to overcome this drawback, the research work presented here does not consider the heuristic mechanism generally adopted and introduces a novel energy utilization function represented as $\epsilon(n)$ to compute the energy utilized during transmissions. The energy utilization function is derived in a manner such that if energy utilization of path between a set of sensor nodes is the least, then the link $l \in L_S$.

b) *Energy Utilization Function $\epsilon(n)$ for Skeleton Extraction*

Let s be a skeleton node and r represent a non-skeleton node. Let $\tilde{f}(n)$ represent a frequency based weight assignment function that assigns skeleton nodes with higher values than the non-skeleton nodes. In other words, $\tilde{f}(s) > \tilde{f}(r)$.

Let's consider sensor node n_{src} at a location $p_{n_{src}} \in \mathcal{A}_{\mathcal{T}}$ transmitting some data to the sensor node n_{dst} located at $p_{n_{dst}} \in \mathcal{A}_{\mathcal{T}}$. If the energy utilized in obtaining the optimal link route is defined as

$$\mathcal{E}(n_{src}) = m \downarrow_{L_{n_{src} n_{dst}}} \int_{n_{src}}^{n_{dst}} \epsilon(L(n)) dn \quad (4)$$

Where $L(n) : [0, \infty) \Rightarrow L^n$ is the function that computes the optimal energy route.
 $L_{n_{src} n_{dst}}$ is the routing table of the sensor node n_{src} to sensor node n_{dst}
 $m \downarrow_{L_{n_{src} n_{dst}}}$ represents the minimum hop route from sensor node n_{src} to sensor node n_{dst}

ϵ represents the energy utilized

The energy utilized in obtaining the optimal route can also put forth the least time interval for any active transmission from n_{src} to n_{dst} when the physical radio layer transmission speed is \mathcal{V} , i.e.,

$$|\nabla \mathcal{E}(n_{dst})| \times \mathcal{V}(n_{dst}) = 1 \quad (5)$$

The energy utilized ϵ with respect to the radio layer transmission rate can be therefore defined as

$$\mathcal{V}(n_{dst}) = 1/\epsilon(n_{dst}) \quad (6)$$

The generalized form of the above equation can be defined as

$$\mathcal{V}(n) = 1/\epsilon(n) \quad (6a)$$

Where $\mathcal{V}(n)$ is the radio layer speed function defined as

$$\mathcal{V}(n) = \chi(\tilde{f}(n)) \quad (7)$$

The skeleton of a 3D sensor network topology consists of a set of nodes S and a set of links connecting these skeleton nodes L_S represented as a graph $\mathbb{G}_S \subset \mathbb{G}$. Let (n_i, n_j) represent a sensor node

pair. The node pair $(n_i, n_j) \in S$ if the energy utilization function is defined as

$$\epsilon(n) = e^{-\eta \tilde{f}(n)} \quad (8)$$

where $\eta > 0$ and is defined as

absolute difference between the neighboring sensor nodes.

$$\eta > (1/\alpha) \ln \left(\sqrt{(d^2x + d^2y + d^2z)} / m \downarrow(dx, dy, dz) \right)$$

c) *S_C point computation*

Where dx, dy, dz is the spacing, $m \downarrow$ is the minimum function and α is the minimum value of the

In the research work presented here, the authors adopt the contour or snake model introduced in Ref.

[43] to obtain the skeleton nodes of the 3D wireless sensor network topology \mathcal{T} . The snake or vector of the trans-

missions that propagate through \mathcal{T} can be defined as

$$V_S(n) = [u_S(n) \ v_S(n) \ w_S(n)]^A \tag{9}$$

The snake $V_S(n)$ minimizes the energy function defined as Eq. (10), yet maintaining topology features

where $f_S(n)$ is the edge map derived, $n = (x, y, z)$ and the parameter of regularization is represented as μ .

$$\mathcal{E}_S(V_S) = \iiint (\mu (|\nabla u_S(n)|^2 + |\nabla v_S(n)|^2 + |\nabla w_S(n)|^2)) + (|f_S(n)|^2 |V_S(n) - \nabla f_S(n)|^2) dn \tag{10}$$

The energy function \mathcal{E}_S of the snake of the V_S is dominated by the partial derivatives of or the primary term in the case where $\nabla f_S(n)$ is small. In the case where $\nabla f_S(n)$ is large, $\mathcal{E}_S(V_S)$ is greatly dominated by the second term and the energy involved can be minimized by assuming $V_S = \nabla f_S(n)$. The use of generalized diffusion equations [44, 45] is considered to find the solution of the snake $V_S(n)$. The $V_S(n)$ of the n^{th} node is

computed from the remaining node points in the topology \mathcal{T} by utilizing a diffusion based procedure and these computations converge to a set of skeleton links $l \in L_S$. The diffusion based procedure is slow by nature and converges towards the center of the topology and in order to compute \mathbb{G}_S , we define the frequency based weight assignment $\mathbf{f}(n)$ as follows where $m \uparrow$ is the max function and $m \downarrow$ is the min function.

$$\mathbf{f}(n) = 1 - ((|V_S(n)| - m \downarrow |V_S|) / (m \uparrow |V_S| - m \downarrow |V_S|))^\omega \tag{11}$$

The parameter ω represents the strength and is assigned values between 0 and 1. The parameter ω is assigned empirically. The weight assignment function defined above enables faster computations and convergence.

the frequency based weight assignment function $\mathbf{f}(n)$. The sensor node with the maximum value of $\mathbf{f}(n)$ is set to be S_C . The computation of S_C is iteratively achieved and if another node whose weight is higher is obtained, then S_C is a new sensor node. The computation of S_C can be defined as

The S_C point is a skeleton node that belongs to all the links defined by L_S and can be obtained based on

$$S_C = \sum_{p=0}^{p=n} (m \uparrow (\mathbf{f}(p))) \tag{12}$$

d) *Skeleton links L_S identification and skeleton node set S construction*

The skeleton links L_S is a set of skeleton links l_s derived from the weight assignment function $\mathbf{f}(n)$. To obtain L_S , the singular skeleton links l_s need to be obtained. Let us consider a skeleton node pair represented by (S_C, S_X) . Let the sensor node S_C initiate a transmission signal to sensor node S_X .

Let l_s represent the skeleton link that exist between the skeleton node pair (S_C, S_X) . The skeleton link l_s is the minimum energy utilized link between the nodes S_C and S_X based on equation (8). Let T be the time taken for the transmission from S_C to S_X . Tracking route reply from S_X to S_C would enable the identification of l_s and this process is defined as

$$S_{n+1} = S_n - h(dT/|dT|), S(0) = S_X \tag{13}$$

where h represents the error step. Using ordinary differential equations, the above equation can be represented as

$$dl/dr = -(dT/|dT|), S(0) = S_X \tag{14}$$

Where r represents the route reply path from S_X to S_C . Adopting the Second order Range-Kutta theorem where the stages $k_1 = f(S_n)$, $k_2 = f(S_n + (h/2)k_1)$ and $f(S_n) = -(dT(S_n)/|dT(S_n)|)$, the above equation can be represented as

$$S_{n+1} = S_n + (h \times k_2) \tag{15}$$

Having obtained a single skeleton link l_s the process is iteratively repeated to obtain the entire skeleton links L_S for all the remaining sensor nodes $s \in S | s \neq S_C$. The iterative process exhibits multiple overlapping links which can be eliminated by tracking the route reply paths. The sensor nodes that exist on the skeleton links are the critical or skeleton nodes and are represented by the set S .

e) \mathbb{G}_S skeleton graph construction

Having obtained the skeleton links L_S and the skeleton node set S , we shall now discuss the methodology adopted in constructing the skeleton graph \mathbb{G}_S . The skeleton graph is obtained by constructing layered topological sets. The layered topological sets are constructed by decomposing the

sensor network topology \mathcal{T} into topological clusters that represent the prominent 3D shape information of the topology. The skeleton sensor node S_C is considered as the root node of the skeleton graph \mathbb{G}_S . Each topological cluster consists of a set of regular sensor nodes and a skeleton node. In other terms, each skeleton node is used to represent a cluster and the skeleton links form the boundary of that cluster. The cluster is identified in terms of the relative distance from the skeleton node S_C . The skeleton graph \mathbb{G}_S is constructed from the layered topological sets, wherein the skeleton nodes represent a cluster and the skeleton links represent the boundaries. On constructing the \mathbb{G}_S ,

it is observed that the leaf nodes of the graph can be used to identify the topological information of the sensor network \mathcal{T} .

The construction of the layered topological clusters is critical to obtain the skeleton graph \mathbb{G}_S without the loss of topological information. Let $Q(n)$ represent the distance function. A transmission with a speed parameter ρ ($\rho > 0$) is propagated from the skeleton node S_C that can be represented as a partial differential equation. The solution of the partial differential equation results in a novel distance function represented as $Q'(n)$. The speed of the transmission is defined as

$$\mathcal{V}(n) = e^{-\rho Q(n)} \tag{16}$$

To derive the function $Q(n)$, it is required to define a parameter ρ . Let us consider a skeleton link $l_S \in L_S$ that exists between two skeleton node pair (S_C, S_X) . Let there exist n regular sensor nodes having $(n - 1)$ links that exist between the skeleton

node pair (S_C, S_X) . Let the skeleton transmit a packet from S_C to S_X with a radio speed represented as ρ . If t_{S_a} represents the time taken to transmit the packets amongst two adjacent sensor nodes, then the time taken to reach the destination can be defined as

$$T = \sum_{a=1}^{n-1} t_{S_a} \tag{17}$$

And t_{S_a} can be defined as

$$t_{S_a} = D(n_{a-1}, n_a) / \mathcal{V}(n_a) \tag{18}$$

Let us consider time t' greater than t_{S_a} , i.e., ($t' > t_{S_a}$) and can define t' as

$$t' \leq D(n_{a-1}, n_a) / e^{\rho f(n_a)} \tag{19}$$

Rearranging the terms of equation (19), ρ can be represented as

$$\rho \leq (1/f(n_a)) \times (\ln(D(n_{a-1}, n_a)/t')) \tag{20}$$

Considering $f(n_a) = f_{m\uparrow}$ and $D(n_{a-1}, n_a) = m \downarrow (dx, dy, dz)$, the value of ρ would result in the worst case scenario. Let ρ' represent the critical value of ρ and can be defined as

$$\rho' \leq (1/f_{m\uparrow}) \times (\ln(m \downarrow (dx, dy, dz)/t')) \tag{21}$$

where $0 < t' < m \downarrow (dx, dy, dz)$ and if $t' = m \downarrow (dx, dy, dz)$ then $\rho' = 0$, which means that the transmission around the S_C skeleton is uniform and if $\rho' = 0$, the layered topological clusters formed are not

accurate. To avoid such scenarios, the authors consider $0 < t' < m \downarrow (dx, dy, dz)$.

The time discretized version of the function $Q'(n)$ is defined as

$$\overline{Q'(n)} = [Q'(n)] \tag{22}$$

Rapid discretization is not considered as $[Q'(n)]$ would not result in accurate layered topological cluster formulations. All the skeleton nodes having the same $\overline{Q'(n)}$ form a cluster provided they are not adjacent to one another. In \mathbb{G}_S , the root node is the topological cluster containing the skeleton node S_C followed by the clusters exhibiting increasing values of $\overline{Q'(n)}$. Two skeleton nodes in the \mathbb{G}_S are said to be connected if there exists a skeleton link amongst them and, the two topological clusters are said to be adjacent if the ancestor skeleton node is common and there exists a skeleton link amongst them.

The identification of the critical sensor nodes or skeleton nodes in the 3D topology \mathcal{T} is represented as a skeleton graph $\mathbb{G}_S(S, L_S)$ consisting of skeleton nodes and skeletal links, which is presented in this section of the paper. The experimental study of the proposed skeleton extraction on varied 3D topologies is discussed in the subsequent section of the paper.

IV. EXPERIMENTAL STUDY

In this section of the paper, the experimental study and the 3D topologies datasets used to evaluate the performance is discussed. The 3D sensor network

viewer is developed using the Windows Presentation Foundation model. The algorithms are developed using C#.Net on the Microsoft Visual Studio platform. The 3D datasets are obtained from the AIM@SHAPE Shape Repository [46]. The points corresponding to the 3D data sets were considered as sensors. The radio ranges of the sensor nodes were varied to achieve complete coverage. The Energy efficient TDMA MAC [47] is considered for communication in the sensor network

topology. The routing protocol is adopted from the paper of Ref. [48]. The experimental analysis presented here discusses the evaluation conducted on a set of five topologies shown in Table 1.

The experimental study presented here consists of 2 sections, namely, skeleton graph G_s construction and performance analysis studied on providing higher energy resources to the skeleton nodes.

Table 1 : Sensor Network Topologies Considered

No	Topology Name	Coverage Area	No Of Sensor Nodes	No Of Skeleton Nodes	No Of Links	Radio Range
1	Genoa Gulf [49]	71910 X 56700 X 1617.77	267	56	3744	7578.9
2	Torus [50]	1 X .32 X.95	50	28	400	0.4
3	Matterhorn [51]	46080 X 46080 X 3524.31	130	36	910	7275.8
4	Naples Gulf [52]	5120 X 5120 X 1347	153	57	2672	1080
5	West Sicily [53]	177570 X 112950 X1130.59	154	39	2852	18937.9

a) G_s skeleton graph construction of wireless sensor network topologies considered

A set of random sensor nodes are deployed on the five topologies considered. The radio range of the sensor nodes is varied to achieve complete coverage over the entire terrain. Homogenous network deployments are considered to construct the skeleton graph G_s . To construct the skeleton graph, first we need to identify the skeletal links L_s and the skeleton node set S . The skeletal link set consists of a number of skeleton links $l \in L_s$. To identify each skeletal link $l \in L_s$, each node is considered as the source and all the other nodes are considered as the destination. The energy utilized $e(n)$ is monitored and the weights are assigned in accordance to the frequency based weight assignment function $f(n)$. The sensor node with the maximum weight $m \uparrow (f(p))$ is considered as the skeleton node S_c . The route reply tracking on the skeleton links and the minimum energy utilized links $l \in L_s$ enables to construct the skeleton node set S . Having obtained the skeleton nodes S and the skeletal links L_s , the skeleton graph needs to be constructed based on the layered topological sets. To construct layered topological sets, the sensor network topology is decomposed into clusters such that each cluster contains only one skeleton node. The distance function $Q(n)$ is computed to obtain the position and location of the cluster represented by the skeleton node in G_s . The skeleton nodes are rearranged to form the skeleton graph G_s centered at the skeleton node S_c .

The experimental study is conducted on varied topology sizes described in Table 1. The results obtained are shown in Table 2. The table shows the terrain views obtained from Ref. [46], sensor deployed, the wireless sensor network topology, skeleton nodes identified and the skeleton extracted.

b) sensor network performance analysis with and without skeleton node considerations

To study the effect of the critical nodes or skeleton nodes, two scenarios are considered in this discussion, namely, "BALANCED" and "PROPOSED SYSTEM" scenario. In the "BALANCED" scheme, a homogeneous sensor network deployment is considered, i.e., all the sensors are assigned with uniform initial power. In the "PROPOSED SYSTEM" scenario, the skeleton nodes identified are assigned an additional energy of about 35% when compared to the other nodes. The networks were simulated and the results were analyzed. The analysis was carried out to study the effect in terms of the network throughput, network overheads and network lifetime.

The results obtained for the Genoa Gulf [49] topology are shown in Figure 5, 6 and 7. The average throughput for the balanced scheme was found to be around 84.9% and for the proposed scheme, it was around 92.7%. The network overheads measured in terms of the energy utilized was reduced by about 44.3%. The efficiency in terms of the network life time is clearly seen in Figure 7.

Table 2 : Proposed Skeleton Extraction in Wireless Sensor Network Topologies

No	Topology Name	Aim@Shape Topology View	Node Deployment View	Sensor Network View	Skeleton Node View	Skeleton Extracted View
1	Genoa Gulf [49]					
2	Torus [50]					
3	Matterhorn [51]					
4	Naples Gulf [52]					
5	West Sicily [53]					

To prove that the skeleton extraction algorithm works well with symmetric topologies, the authors have considered the Torus structure [50]. The results obtained are shown in Figure 8, 9 and 10. The performance improvement in terms of the network throughput, reduction in the network overheads and enhanced network life time is evident from the figures. The Matterhorn mountain terrain [51] is deployed with

130 sensor nodes and the network analysis results obtained is shown in Figure 11- 13. The sensor network analysis obtained considering Naples Gulf [52] and the West Sicily [53] terrain are shown in Figure 14-19. It is observed that the network overhead reduction achieved in Matterhorn is around 22.4%, 41.6% in the case of Naples Gulf and around 20.9% for West Sicily topologies.

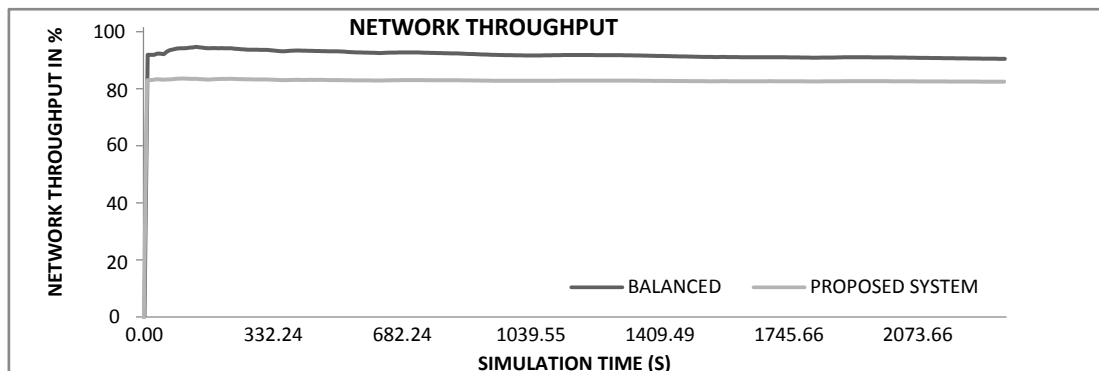


Figure 5 : Network Throughput Analysis for GENOA GULF

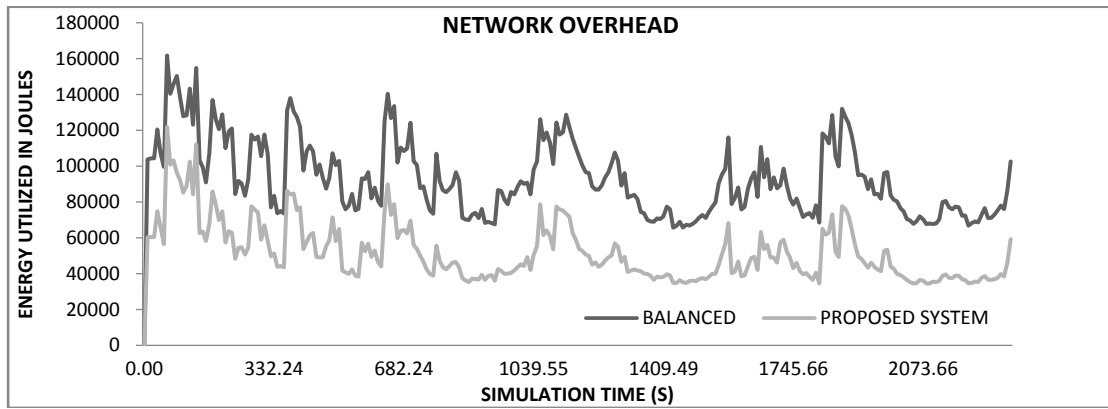


Figure 6 : Network Overhead Analysis for GENOA GULF

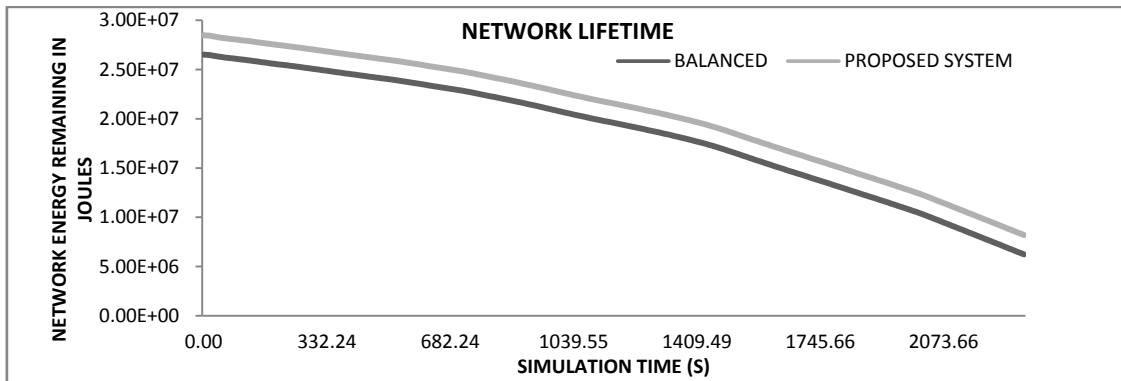


Figure 7 : Network Lifetime Analysis for GENOA GULF

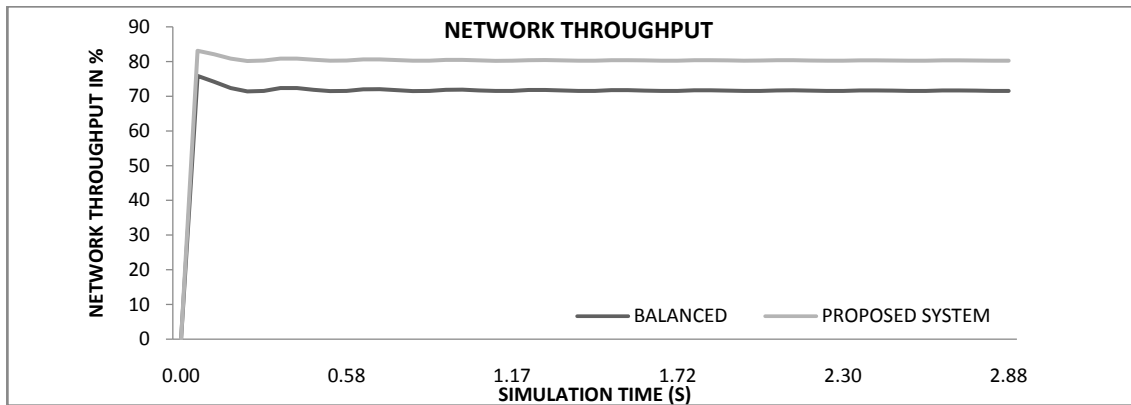


Figure 8 : Network Throughput Analysis for TORUS

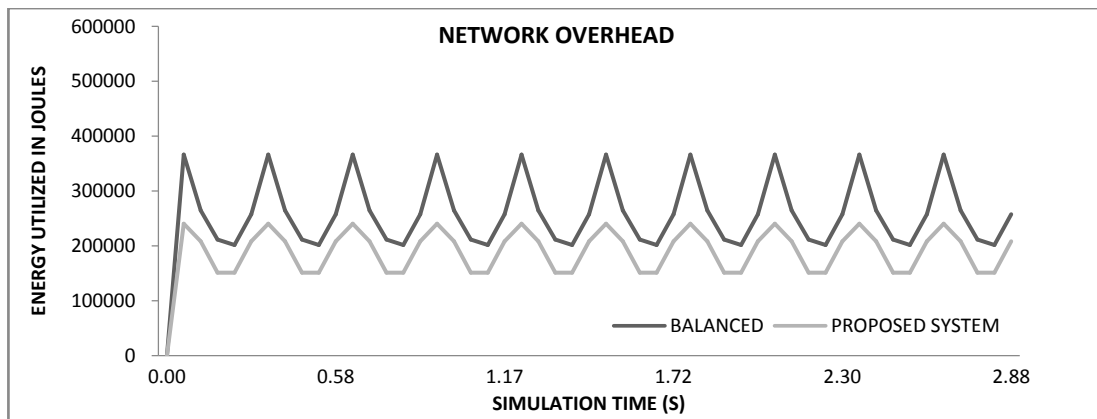


Figure 9 : Network Overhead Analysis for TORUS

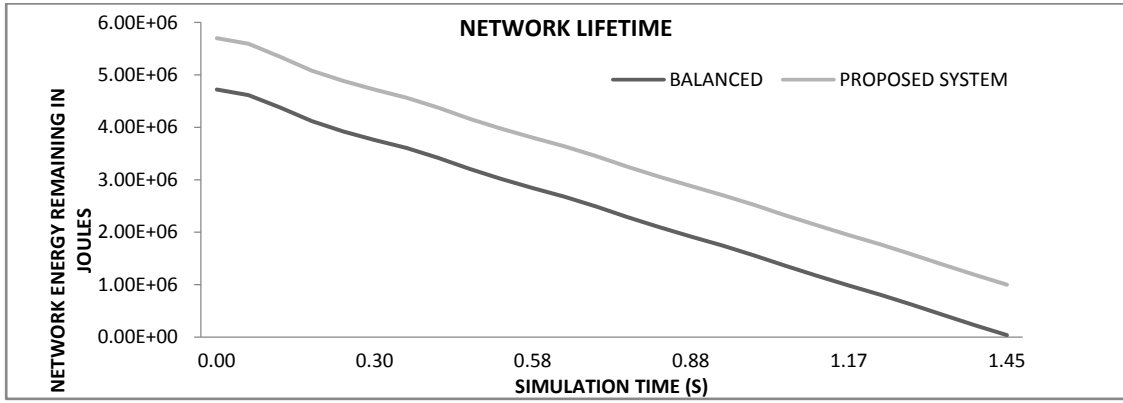


Figure 10: Network Lifetime Analysis for TORUS

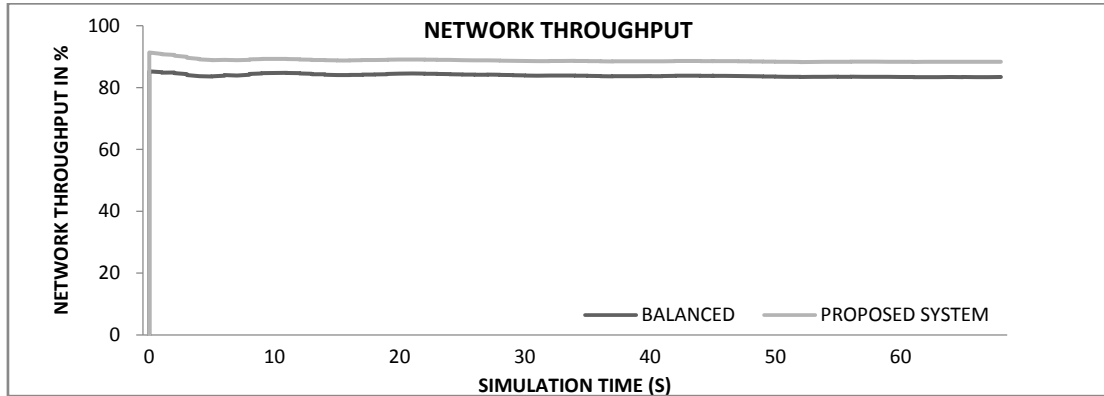


Figure 11: Network Throughput Analysis for MATTERHORN

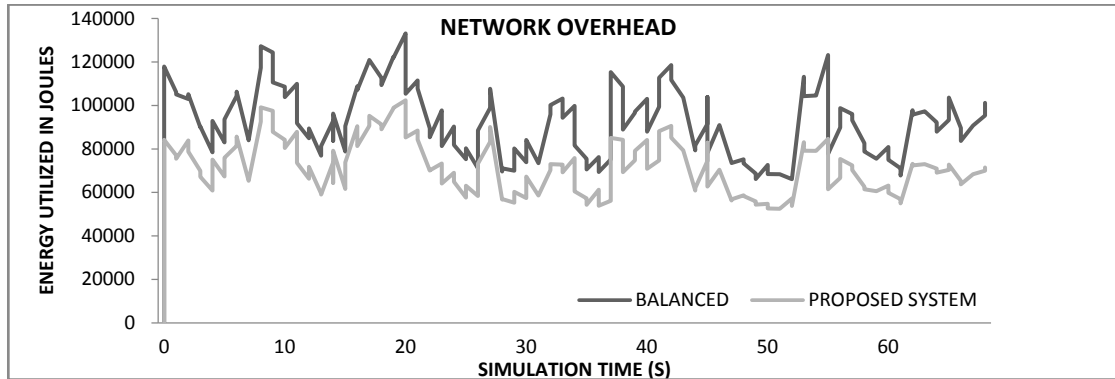


Figure 12: Network Overhead Analysis for MATTERHORN

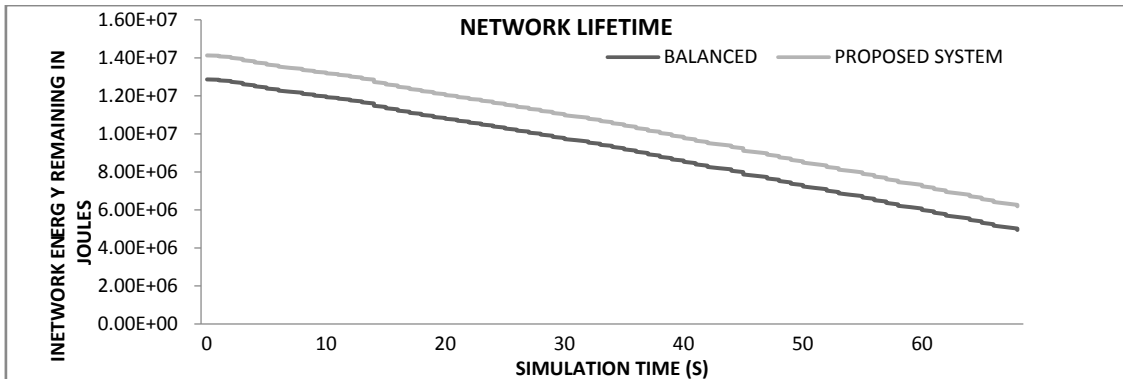


Figure 13: Network Lifetime Analysis for MATTERHORN

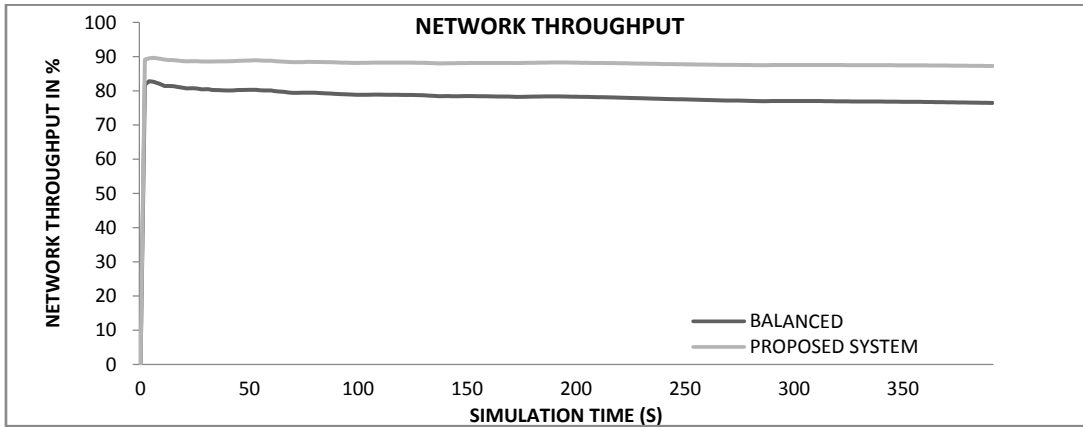


Figure 14 : Network Throughput Analysis for NAPLES GULF

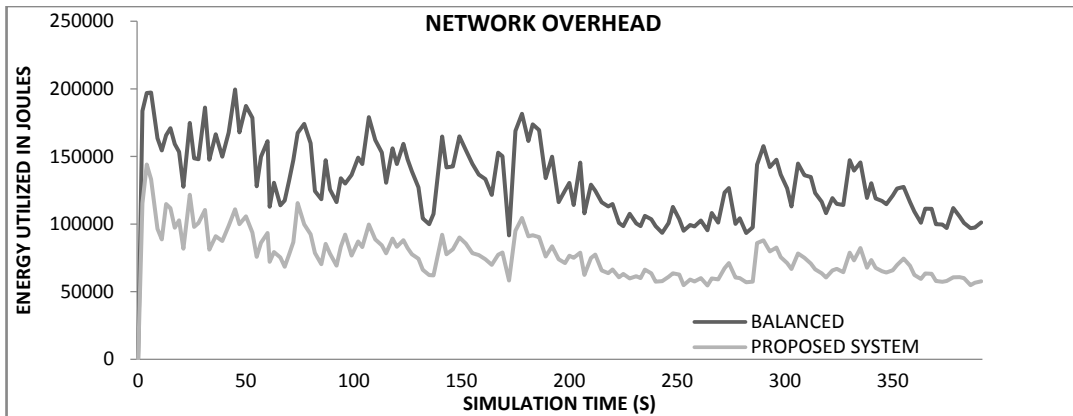


Figure 15 : Network Overhead Analysis for NAPLES GULF

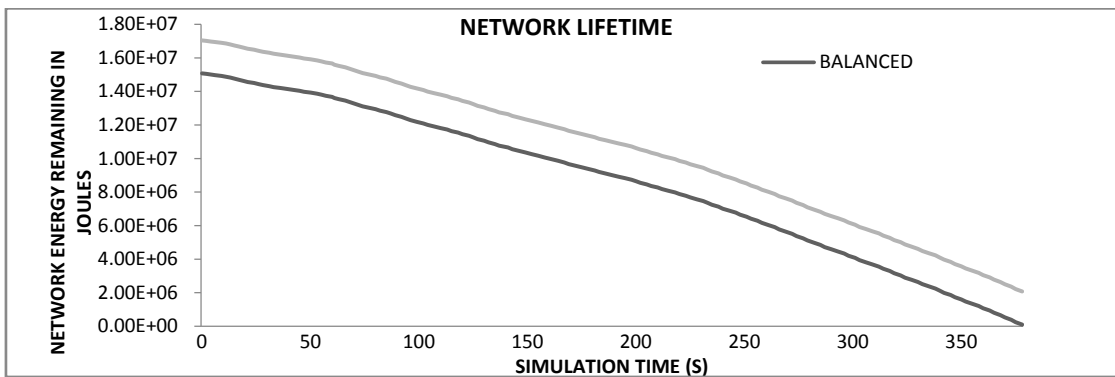


Figure 16 : Network Lifetime Analysis for NAPLES GULF

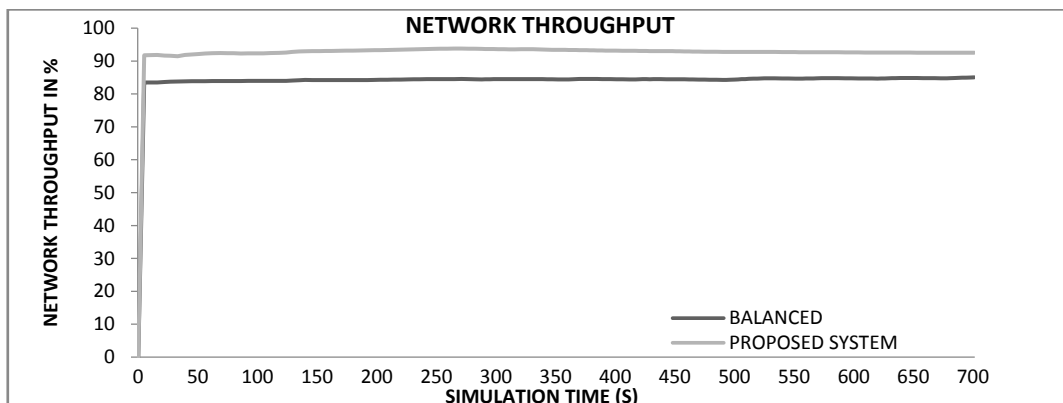


Figure 17 : Network Throughput Analysis for WEST SICILY

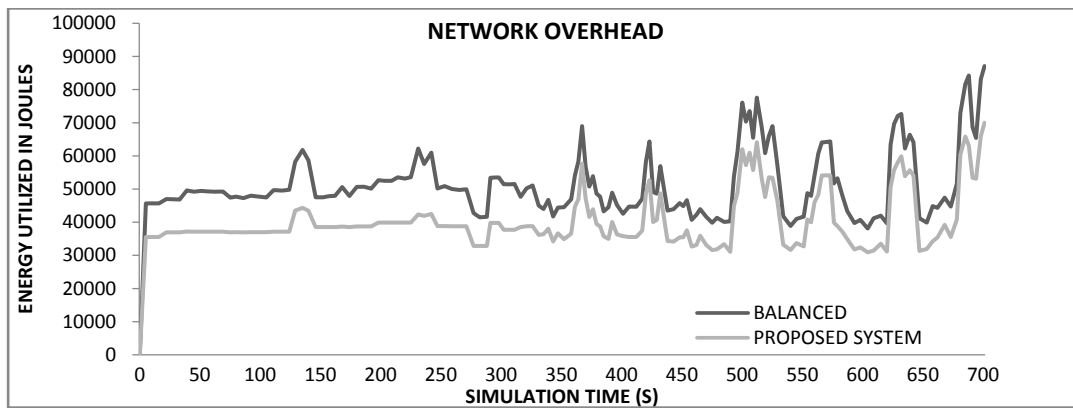


Figure 18 : Network Overhead Analysis for WEST SICILY

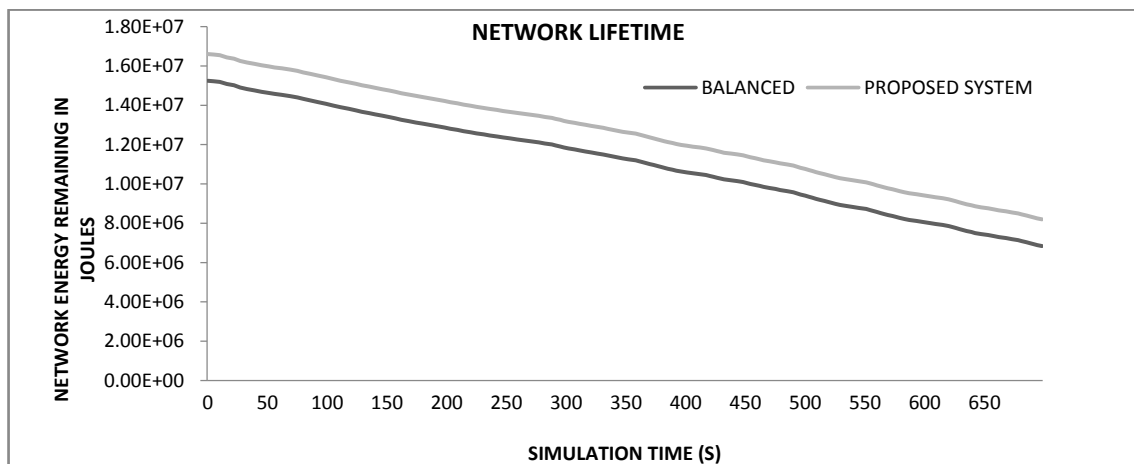


Figure 19 : Network Lifetime Analysis for WEST SICILY

The average throughput of about 88.6% was achieved by the “PROPOSED SYSTEM” when compared to the average throughput of about 80.7% achieved by the “BALANCED” scheme. An average network overhead reduction of about 31.1% was achieved by the “PROPOSED SCHEME”. The network lifetime of the sensor network topology is considerably higher for the “PROPOSED SYSTEM” as additional power is assigned to the skeleton nodes identified. From Figure 5-19, it can be concluded that the “PROPOSED SYSTEM”, wherein additional power resources is provided to skeleton nodes identified achieved better network performance in terms of network throughput, network lifetime and overhead reduction enhancing the efficiency of the wireless sensor network deployments.

V. CONCLUSION

Network design is critical to construct reliable wireless sensor networks. The coverage of 3D sensor networks is complex in nature and the 2D topologies or the 3D projection schemes are not applicable to achieve realistic results. Skeleton extraction and its significance applicable to areas as medical image processing, computer vision, computer graphics and many more are well understood. These skeleton extraction mechanisms

are not applicable to complex 3D wireless sensor networks. Limited work has been carried out to extract the skeleton of 3D wireless sensor networks.

This paper proposes a novel skeleton extraction algorithm applicable to 3D wireless sensor network topologies. The skeleton is represented as a skeleton graph $G_s (S, L_s)$. To construct the skeleton graph each sensor node initiates transmission throughout the network and the energy utilized is monitored. A novel energy utilization function is $e(n)$ is defined to identify the skeletal links L_s . The root node skeleton graph is represented as S_c and is computed based on the frequency based weight assignment function $f(n)$. The skeleton nodes are extracted from the skeletal links and layered topological sets are constructed by adopting a topological clustering mechanism. Each cluster considered consists of one skeleton node and is a part of the skeleton graph. The distance function is computed for each cluster to determine its position in the skeleton node from the root node and the graph G_s is constructed. The skeleton extraction algorithm is validated on a set of varied 3D topologies. Provisioning of additional resources to the skeleton nodes enhances the sensor network performance by 20% and is proved through the experimental study. The results obtained

prove improvements in network throughput, network lifetime and achieve reduction in the network overheads.

VI. ACKNOWLEDGEMENTS

The authors of this paper would like to thank Mr Ashutosh Kumar and Mr Kashyap Dhruve for their valuable suggestion and support.

REFERENCES RÉFÉRENCES REFERENCIAS

1. Tia Gao; Massey T.; Selavo L.; Crawford D.; Borrong Chen; Lorincz, K.; Shnyder, V.; Hauenstein, L.; Dabiri, F.; Jeng, J.; Chanmugam, A.; White, D.; Sarrafzadeh, M.; Welsh, M., "The Advanced Health and Disaster Aid Network: A Light-Weight Wireless Medical System for Triage," *Biomedical Circuits and Systems*, IEEE Transactions on , Vol. 1, No. 3, pp. 203-216, Sept. 2007, DOI: 10.1109/TBCAS.2007.910901.
2. E. Cayirci and T. Coplu, "Sendrom: Sensor Networks for Disaster Relief Operations Management," *Wireless Networks*, Vol. 13, No. 3, pp. 409-423, 2007.
3. I.F. Akyildiz, D. Pompili, and T. Melodia, "Underwater Acoustic Sensor Networks: Research Challenges," *Ad Hoc Networks*, Vol. 3, pp. 257-279, Mar. 2005.
4. R. Szewczyk, E. Osterweil, J. Polastre, M. Hamilton, A. Mainwaring, and D. Estrin, "Habitat Monitoring with Sensor Networks," *Comm. ACM*, Vol. 47, No. 6, pp. 34-40, 2004.
5. M. Fennell and R. Wishner, "Battlefield Awareness via Synergistic SAR and MTI Exploitation," *IEEE Aerospace and Electronic Systems Magazine*, Vol. 13, No. 2, pp. 39-43, Feb. 1998.
6. Patel, S.; Lorincz, K.; Hughes, R.; Huggins, N.; Growdon, J.; Standaert, D.; Akay, M.; Dy, J.; Welsh, M.; Bonato, P., "Monitoring Motor Fluctuations in Patients With Parkinson's Disease Using Wearable Sensors," *Information Technology in Biomedicine*, IEEE Transactions, Vol. 13, No. 6, pp. 864-873, Nov. 2009. DOI: 10.1109/TITB.2009.2033471.
7. Romer, K.; Mattern, F., "The design space of wireless sensor networks," *Wireless Communications*, IEEE , Vol. 11, No. 6, pp. 54-61, Dec. 2004. DOI: 10.1109/MWC.2004.1368897.
8. Hongbo Jiang; Wenping Liu; Dan Wang; Chen Tian; Xiang Bai; Xue Liu; Ying Wu; Wenyu Liu, "Connectivity-Based Skeleton Extraction in Wireless Sensor Networks," *Parallel and Distributed Systems*, IEEE Transactions, Vol. 21, No. 5, pp. 710-721, May 2010. DOI: 10.1109/TPDS.2009.109.
9. Linghe Kong, Mingchen Zhao, Xiao-Yang Liu, Jialiang Lu, "Surface Coverage in Sensor Networks," *IEEE Transactions on Parallel and Distributed Systems*, 25 Feb. 2013. IEEE computer Society Digital Library. IEEE Computer Society, <http://doi.ieeecomputersociety.org/10.1109/TPDS.2012.300>.
10. S. Kumar, T. H. Lai, and A. Arora, "Barrier coverage with wireless sensors". In *ACM MobiCom*, pages 284–298, New York, NY, USA, 2005.
11. X. Bai, D. Xuan, Z. Yun, T. H. Lai, and W. Jia., "Complete optimal deployment patterns for full-coverage and k-connectivity ($k \leq 6$) wireless sensor networks". In *ACM MobiHoc*, pages 401– 410, New York, NY, USA, 2008.
12. M. Watfa and S. Commuri, "A coverage algorithm in 3d wireless sensor networks". *IEEE PerCom*, pages 6 pp. Jan. 2006.
13. C.-F. Huang, Y.-C. Tseng, and L.-C. Lo., "The coverage problem in three-dimensional wireless sensor networks. *IEEE GLOBECOM*, 5:3182–3186 Vol. 5, Dec. 2004.
14. <http://fiji.eecs.harvard.edu/Volcano/>.
15. J.W. Brandt and V.R. Algazi, "Continuous Skeleton Computation by Voronoi Diagram," *CVGIP: Image Understanding*, Vol. 55, No. 3, pp. 329-338, 1992.
16. S. R. Aylward and E. Bullitt, "Initialization, Noise, Singularities and Scale in Height Ridge Traversal for Tubular Object Centerline Extraction," *IEEE Trans. Medical Imaging*, Vol. 21, No. 2, pp. 61-75, 2002.
17. N. Gagvani and D. Silver, "Animating Volumetric Models," *Graphical Models*, Vol. 63, No. 6, pp. 443-458, 2001.
18. Cornea, N.D.; Silver, D.; Min, P., "Curve-Skeleton Properties, Applications, and Algorithms," *Visualization and Computer Graphics*, IEEE Transactions on , Vol. 13, No. 3, pp. 530-548, May-June 2007. DOI: 10.1109/TVCG.2007.1002.
19. N. D. Cornea, D. Silver, and P. Min, "Curve-Skeleton Applications," *Proc. IEEE Visualization Conf. (VIS '05)*, pp. 13-23, 2005.
20. Hongbo Jiang; Wenping Liu; Dan Wang; Chen Tian; Xiang Bai; Xue Liu; Ying Wu; Wenyu Liu, "Connectivity-Based Skeleton Extraction in Wireless Sensor Networks," *Parallel and Distributed Systems*, IEEE Transactions, Vol. 21, No. 5, pp. 710-721, May 2010. DOI: 10.1109/TPDS.2009.109.
21. J. Bruck, J. Gao, and A.A. Jiang, "MAP: Medial Axis Based Geometric Routing in Sensor Networks," *Proc. ACM MobiCom*, 2005.
22. Wenping Liu; Hongbo Jiang; Xiang Bai; Guang Tan; Chonggang Wang; Wenyu Liu; Kechao Cai, "Distance Transform-Based Skeleton Extraction and Its Applications in Sensor Networks," *Parallel and Distributed Systems*, IEEE Transactions on , Vol. 24, No. 9, pp. 1763-1772, Sept. 2013. doi: 10.1109/TPDS.2012.300.
23. X. Zhang, J. Liu, Z. Li, and M. Jaeger, "Volume Decomposition and Hierarchical Skeletonization," *Proc. ACM SIGGRAPH Int'l Conf. Virtual-Reality Continuum and Its Applications in Industry (VRCAI '08)*, pp. 1-6, 2008.

24. T. Wang and A. Basu, "A Note on 'A Fully Parallel 3D Thinning Algorithm and Its Applications'," *Pattern Recognition Letters*, Vol. 28, No. 4, pp. 501-506, 2007.
25. L. Wade and R.E. Parent, "Automated Generation of Control Skeletons for Use in Animation," *The Visual Computer*, Vol. 18, No. 2, pp. 97-110, 2002.
26. T. He, L. Hong, D. Chen, and Z. Liang, "Reliable Path for Virtual Endoscopy: Ensuring Complete Examination of Human Organs," *IEEE Trans. Visualization and Computer Graphics*, Vol. 7, No. 4, pp. 333-342, Oct.-Dec. 2001.
27. H. Sundar, D. Silver, N. Gagvani, and S. Dickinson, "Skeleton Based Shape Matching and Retrieval," *Proc. Shape Modeling Int'l Conf.*, 2003.
28. M. Wan, F. Dachille, and A. Kaufman, "Distance-Field Based Skeletons for Virtual Navigation," *Proc. IEEE Visualization Conf.*, 2001.
29. I. Bitter, A.E. Kaufman, and M. Sato, "Penalized-Distance Volumetric Skeleton Algorithm," *IEEE Trans. Visualization and Computer Graphics*, Vol. 7, No. 3, July-Sept. 2001.
30. J.W. Brandt and V.R. Alazi, "Continuous Skeleton Computation by Voronoi Diagram," *CVGIP: Image Understanding*, Vol. 55, pp. 329-338, 1992.
31. R. Ogniewicz and M. Ilg, "Voronoi Skeletons: Theory and Applications," *Proc. Conf. Computer Vision and Pattern Recognition*, p. 63, 1992.
32. R. Ogniewicz and O. Kubler, "Hierarchic Voronoi Skeletons," *Pattern Recognition*, Vol. 28, No. 3, 1995.
33. Y. Yang, O. Brock, and R.N. Moll, "Efficient and Robust Computation of an Approximated Medial Axis," *Proc. Solid Modeling and Applications Conf.*, 2004.
34. T. Culver, J. Keyser, and D. Manocha, "Exact Computation of the Medial Axis of a Polyhedron," *Computer Aided Geometric Design*, Vol. 21, No. 1, pp. 65-98, 2004.
35. N. Ahuja and J. Chuang, "Shape Representation Using a Generalized Potential Field Model," *IEEE Trans. Pattern Analysis and Machine Intelligence*, Vol. 19, No. 2, pp. 169-176, Feb. 1997.
36. J. Chuang, C. Tsai, and M.-C. Ko, "Skeletonization of Three-Dimensional Object Using Generalized Potential Field," *IEEE Trans. Pattern Analysis and Machine Intelligence*, Vol. 22, No. 11, p. 12-41, Nov. 2000.
37. P. Liu, F. Wu, W. Ma, R. Liang, and M. Ouhyoung, "Automatic Animation Skeleton Construction Using Repulsive Force Field," *Proc. 11th Pacific Conf. Computer Graphics and Applications*, 2003.
38. T. Grigorishin and Y.H. Yang, "Skeletonization: An Electrostatic Field-Based Approach," *Pattern Analysis and Applications*, Vol. 1, pp. 163-177, 1998.
39. W. Ma, F. Wu, and M. Ouhyoung, "Skeleton Extraction of 3D Objects with Radial Basis Functions," *Proc. IEEE Int'l Conf. Shape Modeling and Applications*, 2003.
40. L. Lin and H. Lee, "A Dynamic Medial Axis Model for Sensor Networks," *Proc. IEEE Int'l Conf. Embedded and Real-Time Computing Systems and Applications*, pp. 146-156, Aug. 2007.
41. Hassouna, M.S.; Farag, A.A., "Robust centerline extraction framework using level sets," *Computer Vision and Pattern Recognition*, 2005. *CVPR 2005. IEEE Computer Society Conference on*, Vol. 1, No., pp.458-465, 2005 DOI: 10.1109/CVPR.2005.306.
42. Thomas Deschamps, Laurent D. Cohen, "Fast extraction of minimal paths in 3D images and applications to virtual endoscopy", *Medical image analysis 1 December 2001 (volume 5 issue 4 Pages 281-299 DOI: 10.1016/S1361-8415(01)00046-9)*.
43. Chenyang Xu; Prince, J.L., "Gradient vector flow: a new external force for snakes," *Computer Vision and Pattern Recognition, Proceedings. 1997 IEEE Computer Society Conference on*, Vol., No., pp.66-71, 1997. DOI: 10.1109/CVPR.1997.609299.
44. A.H. Charles and T. A. Porsching. *Numerical Analysis of Partial Differential Equations*. Prentice Hall, Englewood Cliffs, NJ, 1990.
45. C.Xu and J. L. Prince. *Snakes, shapes, and gradient vector flow*. Technical Report JHU-ECE TR96-15, The Johns Hopkins University, Oct. 1996.
46. AIM@SHAPE shape repository. <http://shapes.aim-at-shape.net/>
47. Rong gang Bai; Yu-gui Qu; Yang Guo; Bao-hua Zhao, "An Energy-Efficient TDMA MAC for Wireless Sensor Networks," *Asia-Pacific Service Computing Conference, The 2nd IEEE*, Vol., No., pp.69-74, 11-14 Dec. 2007. DOI: 10.1109/APSCC.2007.25
48. Zussman, G.; Segall, A., "Energy efficient routing in ad hoc disaster recovery networks," *INFOCOM 2003. Twenty-Second Annual Joint Conference of the IEEE Computer and Communications. IEEE Societies*, Vol. 1, pp. 682-691, April 2003 DOI: 10.1109/INFOCOM.2003.1208718.
49. AIM@SHAPE Shape Repository (Sept 18 2013), "Model Name Genoa gulf, ID: 789" Available:<http://shapes.aim-at-shape.net/view.php?id=789>.
50. AIM@SHAPE Shape Repository (Sept 18 2013), "Model name: Torus ,ID: 43" Available : <http://shapes.aim-at-shape.net/view.php?id=43>
51. AIM@SHAPE Shape Repository (Sept 18 2013), "Model name: Matterhorn, ID: 779" Available:<http://shapes.aim-at-shape.net/view.php?id=779>
52. AIM@SHAPE Shape Repository (Sept 18 2013), "Model name: Naples gulf ,ID: 825" Available:<http://shapes.aim-at-shape.net/view.php?id=825>

53. AIM@SHAPE Shape Repository (Sept 18 2013),
"Model name: West Sicily, ID: 879"
Available:<http://shapes.aim-at-shape.net/view.php?id=879>





This page is intentionally left blank